

# The large-scale structure of the Universe in the frame of the model equation of non-linear diffusion

S. N. Gurbatov,<sup>1</sup> A. I. Saichev<sup>1</sup> and S. F. Shandarin<sup>2</sup>

<sup>1</sup>*N. I. Lobachevskii State University, Gor'kii*

<sup>2</sup>*Institute for Physical Problems, Academy of Sciences of the USSR, Moscow and Max-Planck-Institut für Physik und Astrophysik, Institut für Astrophysik, Garching bei München, FRG*

Accepted 1988 July 29. Received 1988 June 6

**Summary.** The evolution of density inhomogeneities and the velocity field in an expanding continuous medium is studied. The consideration is based on the model equation of non-linear diffusion (Burgers' equation), that, together with the equation of continuity incorporating mass density, gives an approximate description of density inhomogeneity growth at the advanced non-linear stage of gravitational instability. The model describes the formation of pancakes, filaments and compact clumps of mass as well as the disruption of the cellular and filamentary structure and the process of merging of the clumps that follows later. At this stage, the statistics of non-linear density peaks, as well as the velocity field, are determined by statistical properties of the fluctuations of the gravitational potential at linear stage. The model is in a sense an extrapolation of Zel'dovich's non-linear solution for gravitational instability of an expanding universe. It does not attempt to describe the internal structure of density enhancements but rather follows the general evolution of inhomogeneities. The model provides an analytic expression for the velocity field and makes it possible to calculate statistical characteristics of an ensemble of density clumps including their masses, velocities and spatial distribution.

## 1 Introduction

In contemporary cosmology there are several models proposed to explain the existence of the large-scale structure (hereafter LSS) of the Universe, which is generally referred to when the spatial galaxy distribution on scales of several tens of Mpc is discussed. In all models, gravitational instability of a homogeneous distribution of mass density plays an important role, but there are models where it is exclusive. In these models the existence of dark matter (hereafter DM) constituting most of the mass in the present Universe is supposed. Moreover, it is also often assumed that the initial perturbations are a small amplitude random field of Gaussian type, which arose at the inflationary stage. The models of this kind have the advantage of being

fully statistically specified by the spectrum of linear density fluctuations. In most papers where the formation of LSS is discussed, a particular spectrum (Harrison–Zel’dovich spectrum) of initial fluctuations is considered. However, other possibilities were found recently (e.g. Kofman & Linde 1987).

At present, in the frame of this theory, most discussions concern two scenarios of LSS formation called hot dark matter (HDM) (e.g. Shandarin, Doroshkevich & Zel’dovich 1983) and cold dark matter (CDM) (e.g. White 1987; Primack 1984) scenarios. These terms reflect the role of thermal velocity dispersion in the evolution of the density-fluctuation spectrum at linear stage.

If the dark matter particles were ‘hot’ they became non-relativistic rather lately. As a result, all perturbations with scales smaller than about  $10^{15} M_{\odot}$  (which approximately equals the horizon scale when HDM becomes non-relativistic) erase due to free streaming. In turn, this means that the first objects to form at the non-linear stage of gravitational instability are pancakes of similar masses; galaxies form later via a fragmentation process.

In the CDM model, density fluctuations can survive down to scales irrelevant to LSS formation; however, the short-wave part of the spectrum becomes suppressed due to a stagnation effect at the radiation-dominated era. The existence of short-wave fluctuations results in the hierarchical clustering scenario for galaxy formation, however, this process could go inhomogeneously with a typical scale of several tens of Mpc. This scale naturally appears in the model, being equal to the comoving horizon size at the epoch when non-relativistic DM becomes the dominating component in the mean density of the Universe and is comfortably close to the scale of observed LSS. Visible manifestation of this scale is definitely connected with the process of galaxy formation which, however, is not very well understood but its real (latent!) cause is the shape of the density-fluctuation spectrum on these scales. If this assumption is true, then the process of galaxy formation plays the role of developing an exposed film.

In this paper we consider the evolution of density perturbations, keeping aside the complicated physics of the galaxy-formation process (Blumenthal *et al.* 1984; Rees 1985; Schaeffer & Silk 1985; Dekel & Silk 1986; Peebles 1986). Moreover, the suggested model in the present form is not supposed to be used to describe the internal structure of non-linear positive-density perturbations. It aims to describe the general evolution of large-scale clumps of mass in terms of their spatial distribution, mass distribution and velocities. In a sense this is an attempt to extend the well known Zel’dovich (1970) approximate solution of non-linear gravitational instability into later non-linear stages, when it fails.

From the cosmological point of view, it provides the possibility of studying some statistical aspects of hierarchical clustering scenarios including (potentially) the complicated case of the CDM model.

Mathematically, the model is based on the equation of non-linear diffusion known as Burgers’ equation (Burgers 1940, 1974). Supplemented with the continuity equation, it describes the evolution of density inhomogeneities in a medium with artificial viscosity. We show later that artificial viscosity can roughly describe the gravitational ‘sticking’ of a collisionless self-gravitating medium in pancakes and other non-linear (in a sense that  $\delta\rho/\rho > 1$ ) objects arising due to gravitational instability (Doroshkevich *et al.* 1980; Dekel 1983). Thus, artificial viscosity is supposed to describe one essential effect of gravitation on small scales, on the other hand the large-scale gravitational effects are supposed to be approximated by the explicit use of Zel’dovich’s solution.

One advantage of using Burgers’ equation is that it has an analytic solution in a very important (from cosmological point of view) case of motions of potential type (i.e.  $\nabla \times \mathbf{v} = \mathbf{0}$ ). Introducing the additional assumption that the viscosity coefficient tends to zero, one can advance in the analysis of some statistical properties of non-linear density distributions by

means of some geometrical technique. The essential feature of this technique is the study of tangential points of the three-dimensional paraboloid with the hypersurface  $\Phi_0 = \Phi_0(\mathbf{q})$  which describes fluctuations of the gravitational potential taken at the linear stage of gravitational instability.

The essential feature of the model is that, analysing the mass distribution at the non-linear stage, it explicitly uses the linear gravitational potential fluctuations rather than density fluctuations (Kofman & Shandarin 1988). It is shown that at the late non-linear stage of gravitational instability many statistical features of the mass distribution directly relate to the statistics and spatial distribution of high peaks of gravitational-potential fluctuations at linear stage.

The general reasons for using Burgers' equation in connection with the problem of LSS formation were discussed in several papers: Gurbatov & Saichev (1984); Gurbatov, Saichev & Shandarin (1984, 1985) and Shandarin (1988).

This paper is organized as follows. In Section 2 we give the explicit derivation of the basic equations used in the model. In Section 3 we discuss the analytic solution of the basic equation. In Section 4 the geometrical interpretation of the solution in the case of infinitely small viscosity is considered. In Section 5 the asymptotic laws of the typical clump-mass growth are derived for power-law spectra of initial fluctuations. In Section 6 some statistical properties of density and velocity fields at the late non-linear stage are discussed. Finally, in Section 7, we present a short summary and discuss prospects.

## 2 Basic equations

We begin with the equations describing the evolution of density inhomogeneities in an expanding dust-like medium written for the density  $\rho$ , the peculiar velocity

$$V_i = u_i - \frac{\dot{a}}{a} r_i = a \frac{dx_i}{dt}, \quad (1)$$

and the perturbation of the gravitational potential  $\phi$  in coordinates comoving with the Hubble expansion of the Universe

$$x_i = r_i/a, \quad (2)$$

where  $r_i$  and  $u_i$  are Eulerian coordinates and velocity,  $a(t)$  is the scale factor and the dot means time derivative. In these variables the equations are (Peebles 1980):

$$\frac{dV_i}{dt} + \frac{\dot{a}}{a} V_i = -\frac{1}{a} \frac{\partial \phi}{\partial x_i},$$

$$\frac{\partial^2 \phi}{\partial x_i^2} = 4\pi G a^2 [\rho(x_i, t) - \bar{\rho}(t)], \quad (3)$$

$$\frac{\partial \rho}{\partial t} + 3 \frac{\dot{a}}{a} \rho + \frac{1}{a} \frac{\partial}{\partial x_i} (\rho V_i) = 0,$$

where  $\bar{\rho}$  is the mean density.

In comoving coordinates Zel'dovich's approximation is:

$$x_i = q_i + b(t) \cdot s_i(\mathbf{q}), \quad (4)$$

where  $x_i$  and  $q_i$  are comoving Eulerian and Lagrangian coordinates respectively;  $b(t)$  is a function of time only describing the evolution of the growing mode of gravitational instability

in linear approximation. In the Einstein–de Sitter cosmological model (with  $\Lambda = 0$  and  $\Omega = 1$ ),  $b(t) \propto a(t) \propto t^{2/3}$ , however, in Friedman’s universe with  $\Omega \neq 1$ ,  $b(t)$  is proportional to the growing solution of the following equation:

$$a\ddot{b} + 2\dot{a}\dot{b} + 3\ddot{a}b = 0. \quad (5)$$

Finally,  $s_i(\mathbf{q})$  is the potential vector field

$$s_i(\mathbf{q}) = \frac{\partial \Phi_0(\mathbf{q})}{\partial q_i} \quad (6)$$

describing the spatial structure of perturbations at linear stage. At this stage, the potential of initial perturbations  $\Phi_0$  relates to fluctuations of the density and the gravitational potential as follows:

$$\begin{aligned} \phi &= 3\ddot{a}ab \cdot \Phi_0(\mathbf{q}), \\ \frac{\rho - \bar{\rho}}{\bar{\rho}} &= -b \cdot \frac{\partial^2 \Phi_0}{\partial q_i^2}. \end{aligned} \quad (7)$$

Assuming that Zel’dovich’s solution is valid outside pancakes, one can calculate the acceleration of every particle explicitly by differentiating (4) twice and substituting  $V_i$  for  $s_i$ :

$$\frac{dV_i}{dt} = \left( \frac{\dot{a}}{a} + \frac{\dot{b}}{b} \right) V_i. \quad (8)$$

Now, introducing new variables

$$\eta(x_i, t) = a^3 \cdot \rho(x_i, t),$$

$$\tilde{v}_i(x_i, t) = \frac{1}{a\dot{a}} \cdot V_i(x_i, t),$$

instead of time  $t$ , density  $\rho$  and velocity  $V_i$ , and putting the explicit expression for the gravitational acceleration (8) into the second equation of system (3) one easily obtains:

$$\frac{\partial \tilde{v}_i}{\partial a} + \tilde{v}_k \frac{\partial \tilde{v}_i}{\partial x_k} = -\frac{1}{a} \left( \frac{\ddot{a}}{\dot{a}} - \frac{\dot{b}}{b} \right) \tilde{v}_i, \quad (9)$$

$$\frac{\partial \eta}{\partial a} + \frac{\partial(\eta \tilde{v}_i)}{\partial x_i} = 0.$$

We do not need the equation for the gravitational potential  $\phi$  any more as we have explicitly used an approximate expression for gravitational acceleration obtained from Zel’dovich’s solution. Before going further, it is worth commenting on the first equation in system (9). The right-hand-side term of this equation recalls by appearance the friction term. However, it can have different signs depending on the sign of the expression in parentheses, which in turn depends on the dimensionless mean density of the Universe. As a result, in open cosmological models, the time-dependent coefficient in front of the velocity is negative and in closed models it is positive. In the former case this means that the expansion of the universe is fast enough to slow down the peculiar motions of matter connected with gravitational instability and, in the

latter case, slow expansion or even contraction of the closed universe promotes the development of the gravitational instability. Both effects are very well known in cosmology.

In the Einstein–de Sitter cosmological model this term cancels since  $b \propto a$ . Thus, the first equation for the velocity  $\tilde{v}_i$  in system (9) describes the ‘inertial’ motion of matter, in an unusual system of variables. Also, for models with  $\Omega \neq 1$  it is possible to reduce system (9) formally to differential equations for inertial motion, by introducing a system of variables involving the perturbation mode  $b(t)$ . Defining new velocities  $v_i$  by

$$v_i(x_i, t) = \frac{\dot{a}}{\dot{b}} \cdot \tilde{v}_i(x_i, t) = \frac{1}{ab} \cdot V_i(x_i, t),$$

we obtain, instead of system (9):

$$\begin{aligned} \frac{\partial v_i}{\partial b} + v_k \frac{\partial v_i}{\partial x_k} &= 0, \\ \frac{\partial \eta}{\partial b} + \frac{\partial(\eta v_i)}{\partial x_i} &= 0. \end{aligned} \tag{10}$$

The systems (9) and (10) are identical in the Einstein–de Sitter cosmological model.

Assuming that at small  $b$  (formally at  $b=0$ ) density is homogeneous, one immediately obtains an evident solution of system (10) in Lagrangian form:

$$\begin{aligned} x_i &= q_i + b \cdot s_i(\mathbf{q}), \\ \eta &= \eta_0 / |\partial x_i / \partial q_k|, \end{aligned} \tag{11}$$

which is Zel’dovich’s solution (4), where  $s_i(\mathbf{q})$  is the initial velocity field. Of course, this is not surprising since to obtain (10) we have used the particular acceleration field calculated from this solution.

Since system (10) is equivalent to Zel’dovich’s approximate solution, it also fails to describe the evolution of density inhomogeneities after the formation of pancakes. An attempt to extrapolate this approximation directly, results in a fast increase in thickness of pancakes but this contradicts the results of numerical simulations of the pancake-formation process. As was first found in one- and two-dimensional numerical simulations (Doroshkevich *et al.* 1980) and later confirmed by numerous three-dimensional simulations, the pancake thickness quickly stabilizes, even in a collisionless medium due to the action of gravity alone. Particles fall into pancakes oscillate about the middle rather than move progressively. At the same time they can drift along the pancake resulting in the formation of filaments and compact clumps.

To overcome this problem, we propose to use the model of ‘sticking particles’. Every particle moves in accordance with the first equation of system (10) until it runs into another one. Then they move together, with the velocity conserving momentum. This model can evidently roughly describe the formation of pancakes as well as filaments and compact clumps of mass. Of course, the inner structure of pancakes and of other objects can not be inferred from the model. The advantage of the model is that it does not allow pancakes to gain thickness unlimitedly. On the other hand, it allows the particles to move along pancakes. Moreover, the model allows the pancakes, filaments and clumps to move as a whole and merge with each other.

In the case of a continuous medium, the model can be described mathematically by inserting the viscous term in the first equation of system (10). Since we do not pretend to describe the



inner structure of mass condensations, this term can be chosen in a simple model form. As we shall see, one of the best forms is that which leads to a three-dimensional equation analogous to the known Burgers' equation (Burgers 1940, 1974). Thus, instead of system (10) we shall use the following:

$$\frac{\partial v_i}{\partial b} + v_k \frac{\partial v_i}{\partial x_k} = \nu \frac{\partial^2 v_i}{\partial x_k^2}, \quad (12)$$

$$\frac{\partial \eta}{\partial b} + \frac{\partial(\eta v_i)}{\partial x_i} = 0. \quad (13)$$

The advantage of using Burgers' equation is connected with the fact that it has an analytic solution that will be discussed in the following section. All considerations below refer to cosmological models with  $\Omega = 1$  as well as  $\Omega \neq 1$ . In the former case, the function  $b(t)$ , playing the role of time in the model, can be replaced by  $a(t)$ .

### 3 Exact and asymptotic solutions of the basic equations

We will consider potential motions only. This agrees with the general idea of the gravitational instability scenario for LSS formation. Indeed it is well known from linear analysis that there is only one growing mode in an expanding Universe which corresponds to motion of potential type.

Let us introduce the velocity potential related to the velocity field as

$$v_i(\mathbf{x}, b) = \frac{\partial \Phi(\mathbf{x}, b)}{\partial x_i}, \quad (14)$$

that, as follows from (12), obeys the following equation:

$$\frac{\partial \Phi}{\partial b} + \frac{1}{2} \left( \frac{\partial \Phi}{\partial x_i} \right)^2 = \nu \frac{\partial^2 \Phi}{\partial x_i^2}, \quad (15)$$

which, by means of Hopf–Cole's substitution,

$$\Phi = -2\nu \ln U, \quad (16)$$

(Hopf 1950; Cole 1951; Kuznetsov & Rozhdestvensky 1961) is transformed to the linear diffusion equation:

$$\frac{\partial U}{\partial b} = \nu \frac{\partial^2 U}{\partial x_i^2}. \quad (17)$$

Now one can easily write the exact solution for equation (12):

$$v_i(\mathbf{x}, b) = \frac{\int \frac{x_i - q_i}{b} \exp \left[ -\frac{1}{\nu} \cdot G(\mathbf{x}, \mathbf{q}, b) \right] d^3 q}{\int \exp \left[ -\frac{1}{\nu} \cdot G(\mathbf{x}, \mathbf{q}, b) \right] d^3 q}, \quad (18)$$

where

$$G(\mathbf{x}, \mathbf{q}, b) = \Phi_0(\mathbf{q}) + \frac{(\mathbf{x} - \mathbf{q})^2}{2b}, \quad (19)$$

and  $\Phi_0(\mathbf{q})$  is the initial velocity potential:

$$v_i(\mathbf{x}, 0) \equiv s_i(\mathbf{q}) = \frac{\partial \Phi_0}{\partial q_i},$$

$\mathbf{q}$  is the Lagrangian coordinate.

We are going to discuss the asymptotic behaviour of solution (18) at small  $\nu$ . At small  $\nu$  the main contribution to the integrals in (18) comes from the vicinity of the point where  $G(\mathbf{x}, \mathbf{q}, b)$  (19) has absolute minimum. One can show that in the limit  $\nu \rightarrow 0$ , solution (18) tends to:

$$v_i(\mathbf{x}, b) = \frac{x_i - q_i(\mathbf{x}, b)}{b}, \quad (20)$$

where  $q_i(\mathbf{x}, b)$  is the coordinate of the absolute minimum of  $G(\mathbf{x}, \mathbf{q}, b)$  at given  $\mathbf{x}$  and  $b$ .

Equation (20) is naturally interpreted in terms of hydrodynamics of a non-interacting medium, with action satisfying equation (15) with  $\nu \rightarrow 0$ . At  $b=0$ ,  $\Phi(\mathbf{x}, 0) = \Phi_0(\mathbf{q})$ , thus, the initial velocity potential is also the initial action; later we shall use both terms. The Eulerian coordinate  $x_i(\mathbf{q}, b)$  of the particle with Lagrangian coordinate  $\mathbf{q}$  (i.e. Eulerian coordinate at  $b=0$ ) changes with time in accordance with equation (11). This means that the velocity at the point with coordinate  $x_i$  at time  $b$  is given by equation (20), where  $q_i(\mathbf{x}, b)$  is the root of equation (11) at chosen  $\mathbf{x}$  and  $b$ . Equation (11) itself is the condition for  $G(\mathbf{x}, \mathbf{q}, b)$  to have a minimum at  $\mathbf{q}$  at chosen  $\mathbf{x}$  and  $b$ :  $\partial G / \partial q_i = 0$ .

At initial linear stage, equation (11) has a single solution. At every point  $\mathbf{x}$  there is only one particle and the velocity field  $v_i(\mathbf{x}, b)$  is single-valued and continuous. Later, however, for some  $\mathbf{x}$ , several roots  $\mathbf{q}_1, \mathbf{q}_2, \mathbf{q}_3$  appear to satisfy equation (11). This means that several particles with different  $\mathbf{q}$  have come to the same point  $\mathbf{x}$  and it takes place in the case of the medium of non-interacting particles. However, solution (20) describes the velocity field of particles sticking at the moment of outstripping. One can find the velocity at such a point from equation (11) if one selects the particle that has not experienced collision up to this time. The other particles which could reach this point, if the medium is collisionless, stuck in pancakes before. If  $\nu \neq 0$ , pancakes have finite thickness but, if  $\nu \rightarrow 0$ , their thickness tends to zero. The selection rule is quite simple. From all the particles reaching the point in the collisionless case one should choose one with the minimal value of  $G(\mathbf{x}, \mathbf{q}, b)$ . At  $\nu \rightarrow 0$  this rule guarantees the conservation of total momentum  $\int \eta v_i d^3x$  (Gurbatov, Saichev & Yakushkin 1983).

#### 4 The formation and evolution of cellular structure at $\nu \rightarrow 0$ . Geometrical formalism

Here we discuss basic qualitative features of the formation and evolution of the structure in the model of sticking matter described by the system of equations (12) and (13). We assume that at the initial state (formally at  $b=0$ ) density is homogeneous and the initial velocity field is given by the potential  $\Phi_0(\mathbf{q})$  connected with the velocity as indicated by (6). The initial potential is supposed to be a smooth random field. To discuss the evolution of the structure we do not need to assume that the potential is a Gaussian random field. At this stage it is enough if it is just generic. However, later, when we discuss some statistical properties of the structure, we assume that it is Gaussian.

Similar to the one-dimensional Burgers' equation (Burgers 1974; Kida 1979; Tatsumi 1980; Gurbatov *et al.* 1983) in the three-dimensional case at  $\nu \rightarrow 0$ , there is a convenient graphic technique to study the velocity field  $v_i(\mathbf{x}, b)$  based on solution (20). It is easy to show that the coordinate of the absolute minimum of  $G(\mathbf{x}, \mathbf{q}, b)$  (19) is also the coordinate of the point where the paraboloid

$$P(\mathbf{x}, \mathbf{q}, b) = -\frac{(\mathbf{x} - \mathbf{q})^2}{2b} + h \quad (21)$$

touches the hypersurface  $\Phi_0(\mathbf{q})$  for the first time while  $h$  grows from  $-\infty$ . Putting the coordinates of the touching  $\mathbf{q}(\mathbf{x}, b)$  into equation (20), one finds the velocity at  $\mathbf{x}$  and  $b$  satisfying equation (12) at  $\nu \rightarrow 0$ .

Discussing the question of touching that takes place in four-dimensional space (three ordinary spatial coordinates plus the value of  $h$ ) we shall call 'point of touching' the point in three-dimensional space ignoring the value of  $h$ . This can be important when we discuss shapes of sets formed by these points. This remark also concerns the top of the paraboloid.

It is worth noting that going on to 'lift' the paraboloid by increasing  $h$ , one can find other points where the paraboloid is tangential to  $\Phi_0(\mathbf{q})$ . Putting their coordinates into equation (20) one can find the velocities of all particles reaching  $\mathbf{x}$  at time  $b$  in the case of a collisionless medium (a one-dimensional illustration is shown in Fig. 1).

Concerning this graphic technique, it is worth mentioning the similarity between gravitational instability in a collisionless medium in the two-dimensional case and geometrical optics (Zel'dovich, Mamaev & Shandarin 1983). The motion of matter in accordance with (4) is like the propagation of beams of light reflecting from a rippled water surface. In this case the initial potential is proportional to the function describing the shape of the surface.

Earlier it was said that we consider smooth initial perturbations. The initial velocity field  $s_i(\mathbf{q})$  is supposed to be statistically homogeneous and isotropic, having typical scale  $L_0$  and rms amplitude  $\sigma$ . It is clear that the kind of touching between the paraboloid  $P$  (21) and the initial potential  $\Phi_0$  depends on their curvatures. The curvature of  $P$  is proportional to  $1/b$  and decreases with time, on the other hand the curvature of  $\Phi_0$  is constant at every point. In fact at every point there are three curvatures determined by the eigenvalues  $\alpha$ ,  $\beta$  and  $\gamma$  of the defor-

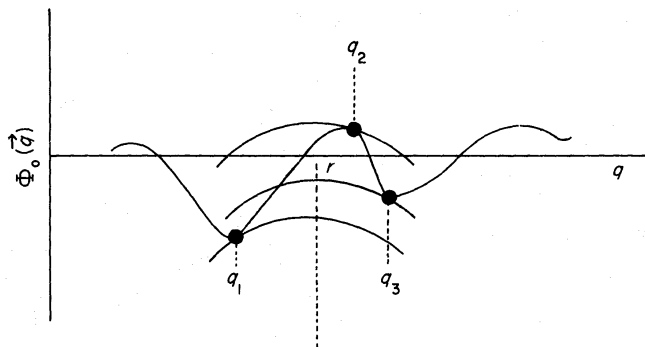


**Figure 1.** One-dimensional illustration of the geometrical technique of the construction of the solution. The horizontal axis is the spatial coordinate ( $x$  or  $q$ ). A wavy curve is the initial potential (action)  $\Phi_0$ . Three positions of the parabola  $P(x, q, b)$ , equation (21), are shown for chosen Eulerian coordinate  $r$ . The points of touching indicate Lagrangian coordinates  $q_1$ ,  $q_2$  and  $q_3$  of particles that would come to  $r$ , if the medium is collisionless. In the frame of Burgers' model only the particle with Lagrangian coordinate  $q_1$  comes to  $r$  at the chosen time  $b$ . The two others stuck into a pancake earlier.



mation tensor  $d_{ik} = \partial^2 \Phi_0 / \partial q_i \partial q_k$  which are assumed to be ordered  $\alpha \leq \beta$ ;  $\beta \leq \gamma$ . As a rough estimate of their magnitude one can take  $\sigma/L_0$ .

While the curvature of the paraboloid  $P$  is greater than that of  $\Phi_0$ , i.e. at  $b < b_0$ , where  $b_0 \sim L_0/\sigma$  is the characteristic time of development of non-linearity, the paraboloid touches the initial potential in a single point  $\mathbf{q} = \mathbf{q}(\mathbf{x}, b)$  at any choice of  $\mathbf{x}$ . This means that at time  $b < b_0$  only one particle with Lagrangian coordinate of the point of touching  $\mathbf{q}$  has come to the Eulerian point with coordinate  $\mathbf{x}$ , i.e., the coordinate of the paraboloid top. Under continuous changing of  $\mathbf{x}$ , the point of touching moves smoothly along the hypersurface of  $\Phi_0(\mathbf{q})$  and the velocity field is continuous at this stage.

However, the paraboloid curvature decreases with growth of  $b$  and the moment comes when it becomes equal to the smallest of the three principal curvatures of the  $\Phi_0(\mathbf{q})$  hypersurface at some point  $\mathbf{q}$ . From pancake theory we know that this point is not a local minimum of  $\Phi_0$  as well as that the eigenvalues can not be equal at such points (Arnol'd, Shandarin & Zel'dovich 1982).

Later, Eulerian space is divided into regions of two kinds. If the coordinate of the paraboloid top  $\mathbf{x}$  is in a region of the first kind, it can touch the hypersurface  $\Phi_0(\mathbf{q})$  only at one point, otherwise it can do it at three points at different  $h$  (Fig. 1). However, in the latter case, there is only one point  $\mathbf{q}$  corresponding to the smallest  $h$  when the paraboloid touches  $\Phi_0(\mathbf{q})$  without intersecting it at other points. This point corresponds to the particle that has reached the Eulerian point in question 'safely' and two others stuck in a pancake earlier. The velocity at this Eulerian point equals the velocity of the first particle.

In addition, the paraboloid can touch the hypersurface  $\Phi_0(\mathbf{q})$  in two points simultaneously (a one-dimensional illustration is shown in Fig. 2). The case of 'double-touching' is degenerate and therefore the set of points with coordinates of the paraboloid tops, when the double-touching takes place, is of less dimensionality. Initially it forms pieces of surface (sheets) in three-dimensional Eulerian space.

Shortly after appearance, the set of double-touching points forms a closed surface in Lagrangian space. Points enclosed by the surface can not be touched by the paraboloid if we hold the agreement that intersection of  $\Phi_0$  is not allowed (Fig. 2). The mass of matter enclosed by the surface is the mass of the sheet. The three-dimensional density of the sheet tends to infinity if  $\nu \rightarrow 0$ .

While  $b$  grows, the region enclosed by the surface of double-touching increases in Lagrangian space and therefore increases the mass of the sheet as well as its size. Other sheets are originated by the other minima of  $\Phi_0$ .

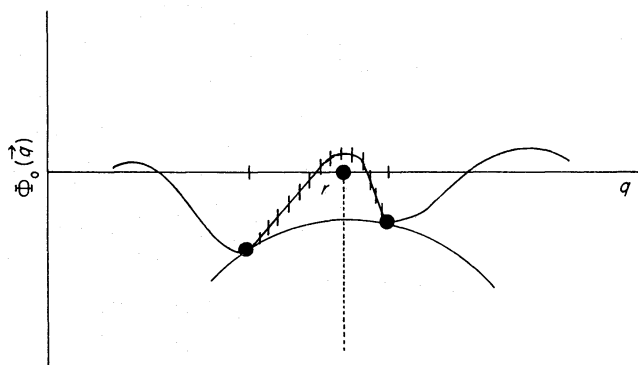


**Figure 2.** One-dimensional illustration for the geometrical finding of the pancake coordinate  $r$ . The critical position of the parabola touching  $\Phi_0$  at two points simultaneously is shown. The marked interval between the Lagrangian coordinates of the points of touching indicate the matter stuck into the pancake by this time.

The next stage in the evolution of the structure begins when paraboloids appear which touch the hypersurface  $\Phi_0$  in three points simultaneously. The appearance of triple-touching is connected with intersections of sheets along the ribs.

Finally, the last type of touching appears. In this case the paraboloid touches the hypersurface at four points simultaneously. Thus, the apices where the ribs intersect appear. This completes the formation of the cellular structure. After this stage, the qualitative character of the structure does not change. However, very important quantitative changes occur.

First, the typical size of cells grows because one cell swallows up the others. And second, the fractions of mass in different elements of the structure (i.e. voids, sheets, ribs and apices) change dramatically with the general trend of mass migration from voids to sheets then to ribs and then to apices. Finally, practically all the mass is concentrated in apices and one can speak about cellular structure quite relatively. One can equally say that cellular structure is destroyed at this stage. However, in a continuous medium, the cellular structure formally exists forever in a sense that we shall discuss later.

Now let us consider the asymptotics of the evolution of the structure (see also Gurbatov & Saichev 1981). At  $b \gg b_0$ , the top of the paraboloid becomes very flat compared with the shape of peaks of the initial potential  $\Phi_0$ . Therefore the paraboloid touches the hypersurface  $\Phi_0$  practically at its minima and finally at the deepest ones. Thus the asymptotic behaviour of the system is controlled by the statistics and spatial distribution of the deepest troughs of the initial potential  $\Phi_0$ . The importance of studying the statistics of peaks in Gaussian fields, however, in a different context, has also been stressed by Peacock & Heavens (1985) and Bardeen *et al.* (1986). The absolute minimum of  $G(\mathbf{x}, \mathbf{q}, b)$  [see (18) and (19)] practically coincides with one of the local minima of  $\Phi_0$ . The coordinate of the absolute minimum of  $G(\mathbf{x}, \mathbf{q}, b)$  becomes a step function of  $\mathbf{q}$  which is practically constant in separate regions  $\Sigma_i$  and is breaking at their boundaries. Inside every region the velocity field approximately equals

$$\mathbf{v}(\mathbf{x}, b) = \frac{\mathbf{x} - \mathbf{q}_i}{b}, \quad \mathbf{x} \in \Sigma_i, \quad (22)$$

where  $\mathbf{q}_i$  is the coordinate of the corresponding minimum of  $\Phi_0$ . Strictly speaking the coordinate of the touching point changes a little at different  $\mathbf{x}$  in this region but at  $b \gg b_0$  the distance between the point of touching and the coordinate of the minimum is small.

Regions  $\Sigma_i$  with universal structure of the velocity field (22) we will call 'cells'. Now, every cell is characterized by its 'centre'  $\mathbf{q}_\alpha$  and its value of initial action  $\Phi_\alpha \equiv \Phi_0(\mathbf{q}_\alpha)$ . In every cell matter moves from the 'centre'  $\mathbf{q}_\alpha$ , resulting in the formation of the cellular structure. However, the 'centre' of the cell can be situated outside the cell.

The walls between the cells are determined by the condition of touching of the paraboloid (21) with the initial action  $\Phi_0$  in two points simultaneously. At  $b \gg b_0$ , these points are close to two cell centres  $\mathbf{q}_\alpha$  and  $\mathbf{q}_\beta$ ; thus, the boundary between them  $\mathbf{x}_{\alpha\beta}$  satisfies the equation  $G(\mathbf{x}_{\alpha\beta}, \mathbf{q}_\alpha, b) = G(\mathbf{x}_{\alpha\beta}, \mathbf{q}_\beta, b)$  which can be transformed to the following one:

$$\left( \mathbf{x}_{\alpha\beta} - \frac{\mathbf{q}_\alpha + \mathbf{q}_\beta}{2} \right) (\mathbf{q}_\alpha - \mathbf{q}_\beta) = b \cdot (\Phi_\alpha - \Phi_\beta). \quad (23)$$

One can see from this equation that the walls of the cells are planes perpendicular to the vector  $\mathbf{q}_\alpha - \mathbf{q}_\beta$ ; their velocities are constant, parallel with  $(\mathbf{q}_\alpha - \mathbf{q}_\beta)$ , proportional to the difference of the actions  $(\Phi_\alpha - \Phi_\beta)$  and directed from the centre of the cell having smaller action. The walls intersect along straight ribs which in turn intersect in common apices of cells. The velocity field has breaks at the walls; at  $b \gg b_0$  the surfaces of the velocity break form a single connected structure.

The distribution of density inside cells can be found by solving the continuity equation (13) with the velocity field found from equation (12). However, it is more convenient to study the picture of the density distribution qualitatively, and sometimes also quantitatively, following the evolution of the elementary volume, i.e., the Jacobian of the transformation from Lagrangian  $\mathbf{q}$  to Eulerian  $\mathbf{x}$  coordinates. The density in the vicinity of the Lagrangian point  $\mathbf{q}$  equals:

$$\eta = \frac{\eta_0}{|\delta_{ik} + b \cdot d_{ik}|}; \quad d_{ik} = \partial^2 \Phi_0 / \partial q_i \partial q_k, \quad (24)$$

where  $\eta_0$  is the initial density;  $\delta_{ik} = 1$  if  $i = k$  and 0 otherwise. Inside the cells the matter moves in accordance with (11), this gives us the opportunity to estimate the density. At  $b \gg b_0$  in Lagrangian space every cell represents a small isolated 'island' including a minimum of the initial action  $\Phi_0$  (Fig. 3). The fact that, due to continuous swallowing up of cells, only cells with deepest minima of  $\Phi_0$  can survive, allows us to estimate the density inside cells. It is much more difficult to estimate the density distribution inside the walls, since the trajectories of the corresponding particles are very complicated. However, some qualitative conclusions can be done by studying the behaviour of particles fallen into the walls. To do this one needs to consider the structure of the walls at small but finite  $\nu$ . The analysis of competition of initial

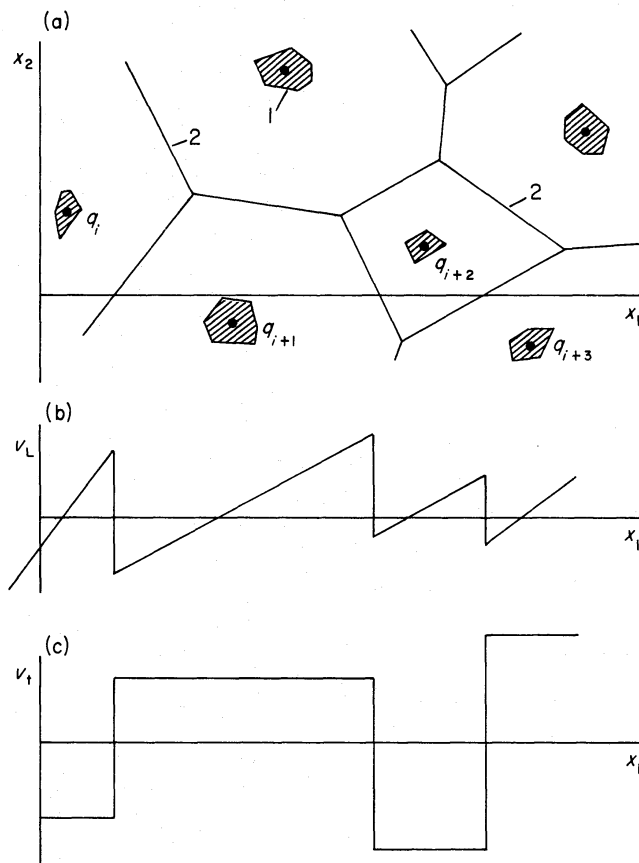


**Figure 3.** Two-dimensional illustration of the asymptotic structure of the density and velocity fields. The cellular structure is schematically shown in (a). Lines show the walls where density is infinite (at  $b \gg b_0$ ) and the velocity field has breaks. Hatched 'islands' placed about the minima of the initial action  $\Phi_0$  indicate the region in Lagrangian space the matter from which has not yet stuck into pancakes. (b) and (c) show the distribution of longitudinal  $v_L$  and transverse  $v_t$  velocities along the  $x_1$ -axis.

actions between neighbouring cells leads to the following equation for the velocity field in the vicinity of the walls:

$$\mathbf{v}(\mathbf{x}, b) = \frac{1}{b} \left( \mathbf{x} - \frac{\mathbf{q}_\alpha + \mathbf{q}_\beta}{2} \right) - \frac{\Delta \mathbf{q}_{\alpha\beta}}{2b} \operatorname{th} \left( \frac{\Delta \mathbf{q}_{\alpha\beta} (\mathbf{x} - \mathbf{x}_{\alpha\beta})}{4\nu \cdot b} \right), \quad (25)$$

where  $\Delta \mathbf{q}_{\alpha\beta} = \mathbf{q}_\alpha - \mathbf{q}_\beta$ . Thus, at finite  $\nu$ , the velocity field has two scales: external  $L(b)$  characterizing the typical size of cells and internal  $l(b)$  connected with the external one by the following relation:

$$l(b) \sim \frac{\nu \cdot b}{L(b)}, \quad (26)$$

characterizing the thickness of the walls. It is worth remembering that the density distributions in pancakes arising in a collisionless medium or in a gas are quite different from those arising in the model in question, even at  $\nu \neq 0$ . This discussion explains only what happens at finite  $\nu$ .

Trajectories of individual particles  $\mathbf{x}(b)$  satisfy the following equation:

$$\frac{d\mathbf{x}}{db} = \mathbf{v}(\mathbf{x}(b), b), \quad (27)$$

where the velocity field is determined by equation (12). Using it, one can find the force acting on the particle:

$$\frac{dx_i}{db} = v_i,$$

$$\frac{dv_i}{db} = F_i(\mathbf{x}(b), b), \quad (28)$$

$$F_i(\mathbf{x}, b) = \nu \cdot \frac{\partial^2 v_i(\mathbf{x}, b)}{\partial x_k^2}.$$

The analysis of (25) and (28) shows that the motion of the particle consists of two stages. Inside the cell it moves freely in accordance with (11). In common physical variables the particle moves in agreement with the theory of gravitational instability. However, when it approaches the wall at a distance about  $l$ , the restraint force directed normally to the wall emerges. Due to this force, the normal velocity of the particle relative to the wall decreases and finally becomes equal to zero.

The tangential component of the velocity is conserved and the particles fallen on to a wall continue to move from its centre to the ribs. Afterwards, the matter moves along the ribs to the apices of the cells. One should not think that the walls, ribs and apices are at rest. They also move, resulting in the swallowing up of some cells and merging of apices. This is how the structure evolves.

## 5 The asymptotic growth of the scale of the structure

The motion of the walls changes the cell shapes continuously. As the velocity field is directed from the cells with deeper minima of the initial action  $\Phi_0$ , these cells swallow up their

neighbours, resulting in the growth of the external scale of the structure  $L(b)$ . The growth of  $L(b)$  is determined by the initial conditions.

We now discuss the dependence of the growth of the external scale  $L$  from the spectrum  $\Delta_k^2$  of the initial action  $\Phi_0$ , assuming that it is a random Gaussian field. However, in cosmology, the problem of LSS formation is discussed mostly in terms of the spectrum  $\delta_k^2$  of linear density perturbations  $\delta\rho/\rho$ . Because of equation (7), the spectrum  $\Delta_k^2$  relates to  $\delta_k^2$  as

$$\Delta_k^2 \propto k^{-4} \cdot \delta_k^2. \quad (29)$$

We suppose that  $\Delta_k^2$  has a cut-off of some kind (exponential or a power law) at  $k \rightarrow \infty$ , i.e., at short waves. In the case of the HDM model it is evidently justified because of free-streaming damping of short-wave perturbations at relativistic stage. For the others, including the CDM model, we just assume that the scale of the cut-off  $L_0$  is much smaller than that under consideration in the non-linear regime  $L \gg L_0$ . In long waves  $k \rightarrow 0$ , the spectrum  $\Delta_k^2$  is supposed to be a power law

$$\Delta_k^2 \propto k^{n-4}. \quad (30)$$

We keep the notation  $n$  for the spectral index of the density perturbation spectrum which is common in cosmology:  $\delta_k^2 \propto k^n$ .

The rate of growth  $L(b)$  is different depending on whether the dispersion of the initial action  $\Phi_0$  is finite  $\langle \Phi_0^2 \rangle = \sigma_\Phi^2 < \infty$  or diverges at  $k \rightarrow 0$  as

$$\Delta_k^2 \propto \kappa^2 k^{n-4}, \quad \kappa = \text{const}, \quad (-1 < n < 1). \quad (31)$$

One can see from (19) that a local minimum of the initial action  $\Phi_0$  can be an absolute minimum of  $G(\mathbf{x}, \mathbf{q}, b)$  if it is not weighed too highly by the parabolic term. The characteristic scale of the region where an absolute minimum can exist can be found by comparing the increases of the paraboloid with the initial action. This leads to the following equation for  $L(b)$  (Gurbatov & Saichev 1981):

$$L^2(b) \sim 2b\sqrt{D[L(b)]}, \quad (32)$$

where  $D(x)$  is a structural function for  $\Phi_0$ :

$$D(x) \equiv \langle [\Phi_0(x) - \Phi_0(0)]^2 \rangle. \quad (33)$$

In the first case when  $D(x \gg L_0) \approx 2\sigma_\Phi^2$  one gets:

$$L(b) \sim \sqrt{\sigma_\Phi \cdot b} \sim L_0 \left( \frac{b}{b_0} \right)^{1/2}. \quad (34)$$

In this case, the growth of the typical cell-size depends only on the integral characteristics of the initial spectrum and not on its peculiarities.

In the second case (31), when  $D(x) \sim \kappa^2 x^{(1-n)}$  at  $(-1 < n < 1)$ , (32) gives:

$$L(b) \sim \sqrt{\kappa} \cdot b^{2/(n+3)}. \quad (35)$$

The physical reason for this difference is that in the second case there is a long distance correlation between the values of  $\Phi_0$  and in the first one there is not. Comparing (34) and (35) one can see that the existence of long distance correlation speeds up the growth of the cell-scale.

Using (34) and (35) one can roughly estimate the growth of the characteristic clump mass, supposing that at this stage most of the mass is in clumps and therefore  $M_L \sim \eta_0 L^3$ . In the first case (34) [in (30)  $n > 1$ ]:



$$M_L \sim M_0 \cdot b^{3/2}, \quad (36)$$

independently of the particular value of  $n$ , and in the second case (35) [ $\ln(30) - 1 < n < 1$ ]:

$$M_L \sim M_0 \cdot b^{6/(n+3)}, \quad (37)$$

We should stress that the last formula is in agreement with the prediction of the hierarchical clustering model (see, for example, Peebles 1980). However, the prediction of the model in question for clump-mass evolution in the case of steep initial spectra [ $n > 1$ , formula (37)] is quite different.

It was recognized long ago that non-linearity can affect the evolution of the long-wave part of the density-perturbation spectrum. Press & Schechter (1974) and then Doroshkevich & Zel'dovich (1975) came to the conclusion that there is a limit rate for clump-mass evolution:  $M \propto a^{6/7}$  in a  $\Omega = 1$  model, independent of the particular value of the density spectrum index  $n$ , if  $n > 4$ . This comes from the non-linear generation of the long-wave part of the spectrum, even in the linear regime of density-perturbation evolution. Thus, even if there are no long-wave perturbations at linear stage, all the clump mass will grow at these scales steadily with the limit rate mentioned above. However, there is a general belief that if  $-3 < n < 4$  then formula (37) holds.

The model suggested here claims that, although the limit rate of the clump-mass growth does exist, it is faster and holds in a wider range of power-law spectrum indices (34) ( $n > 1$ ) than it was thought before. The final solution of this discrepancy might come from direct numerical simulations of the gravitational instability at late non-linear stage but the problem does not seem to be simple in the three-dimensional case. The first attempt to find this effect in one-dimensional numerical simulations has given the evidence approving it (Kotok & Shandarin 1988), however, one must remember that both the limit rate of clump-mass growth and the range of spectrum indices depend on the dimensionality of space.

Concerning the other restriction imposed on the familiar law (37), i.e.,  $n > -1$ , at present we can say little. The analysis used in other cases is not formally applicable here because of too-strong long-distance correlation of values of  $\Phi_0$ . It is probably a manifestation of strong influence of the long-wave part of the initial spectrum on the structure evolution, even when much shorter scales become non-linear. This means that if the slope of the spectrum becomes flatter on some scale, then this scale manifests itself in the inhomogeneous distribution of smaller clumps. If there is no such change of the spectrum, then the structure formation cannot be considered as a statistically homogeneous process.

## 6 Asymptotic analysis of some statistical properties of density and velocity fields

More complete analysis is possible in the first case when the condition of full mixing is fulfilled, that means that the correlation function of the initial action  $\langle \Phi_0(\mathbf{x}_0) \cdot \Phi_0(\mathbf{x} + \mathbf{x}_0) \rangle$  decreases quickly at distances much larger than the scale of the initial perturbations  $x \gg L_0$ . It is possible due to the existence of a small parameter  $\varepsilon = L_0/L(b) \ll 1$  at  $b \gg b_0$ . At  $L \gg L_0$  the field at any point is determined as a result of the competition between the numerous local minima of the initial action  $\Phi_0$  that permits us to use the limit theorems of probability theory. Here we discuss only the more important results of the analysis, a more detailed study of this problem can be found in a separate paper by Gurbatov & Saichev (1981).

First of all it is worth noting that at  $L(b) \gg L_0$  the random field  $\mathbf{v}(\mathbf{x}, b)$  becomes statistically self-similar, that means that all its statistical properties depend only on one scale  $L(b)$ . At  $b \gg b_0$ , the external scale of the structure  $L(b)$  is very close to the rough estimate (34) and equals

$$L(b) = \sqrt{\sigma_\Phi \cdot b \left( \frac{\sigma_\Phi}{h_0} \right)} \approx \sqrt{\frac{L_0 \sigma b}{\sqrt{3 \ln(\sigma b/L_0)}}}, \quad (38)$$

where  $\sigma$  and  $\sigma_\Phi$  are the dispersions of the initial velocity  $\mathbf{s}(\mathbf{q})$  and action  $\Phi_0$  fields, and  $h_0$  is the characteristic value of the absolute minimum of  $G$

$$h_0 \approx \sigma_\Phi \sqrt{3 \ln(\sigma b/L_0)}. \quad (39)$$

The growth of  $h_0$  with time is connected with an increasing number of minima of  $\Phi_0$  competing to become the deepest. It is assumed that  $h_0 \gg \sigma_\Phi$ .

It is also possible to show that at  $b \gg b_0$  only particles having the initial action  $\Phi_0$  in the rather narrow range  $\Delta h \sim \sigma_\Phi / \sqrt{3 \ln(\sigma b/L_0)}$  about the characteristic value  $h_0$  (39) have a chance of survival (i.e. do not stick into a clump). This can be used for an estimation of the mean density inside cells. Really to find the density one needs to average (24) using the conditional probability

$$w_0(d_{ij} | -h_0) \equiv w_0(d_{ij}, -h_0) / w_0(-h_0), \quad (40)$$

where  $w_0(d_{ij}, h)$  is the joint distribution of  $d_{ij}$  and  $\Phi_0$ . At  $b \gg b_0$  ( $h_0 \gg \sigma_\Phi$ ), the conditional mean value of diagonal elements of the tensor  $d_{ii}$  is much greater than its dispersion and thus the mean density inside the cells is approximately equal to

$$\langle \rho \rangle \approx \rho_0 \left( \frac{b_0}{b} \right)^3 \left[ \ln \left( \frac{b_0}{b} \right) \right]^{-3/2}. \quad (41)$$

The characteristic volume of cells increases with time because of swallowing up of some cells, but of course the mean mass contained in a cell decreases as  $\rho_0 L_0^3 (b_0/b)^{3/2}$  since more mass is accumulated in clumps situated in the apices of the cells.

As follows from asymptotic analysis at  $b \gg b_0$ , the probability distribution of  $\mathbf{v}(\mathbf{x}, b)$  is Gaussian, with dispersion  $\sim L^2(b)/b^2$ . On the contrary, the two-point distribution  $w_2(\mathbf{v}_1, \mathbf{v}_2, \mathbf{x}_1, \mathbf{x}_2, b)$  [where  $\mathbf{v}_1 = \mathbf{v}(\mathbf{x}_1, b)$  and  $\mathbf{v}_2 = \mathbf{v}(\mathbf{x}_2, b)$ ], keeping information about correlation properties of  $\mathbf{v}(\mathbf{x}, b)$  and permitting the detailed study of the cellular structure, is not Gaussian. Asymptotically, it can be represented at  $b \gg b_0$  as

$$w_2 = pV + (1-p)W, \quad (42)$$

where  $V$  is the two-point distribution function under the condition that the points  $\mathbf{x}_1$  and  $\mathbf{x}_2$  are in the same cell, and  $W$  is also the two-point distribution, but the points are in different cells, and  $p$  is the probability that two points are in the same cell.

The two-point distribution permits the study of probability distribution of both longitudinal  $v_l = \mathbf{v} \cdot \mathbf{n}$  [where  $\mathbf{n} = (\mathbf{x}_1 - \mathbf{x}_2) / |\mathbf{x}_1 - \mathbf{x}_2|$ ] and transverse components  $v_t$  of the velocity field, as well as their correlation functions and spectra. It turns out that the two-point distribution function of the radial component is the same in space of arbitrary dimensionality (1, 2 or 3) and coincides with the distribution for Burgers' one-dimensional turbulence (Gurbatov & Saichev 1981). Transversal components are statistically independent in different cells and have a Gaussian distribution function.

Normed correlation functions for longitudinal  $R_{ll}$  and transverse  $R_{tt}$  components of the velocity field can be expressed by means of the probability of two points being in the same cell:

$$R_{ll}(2s) = \left( \frac{b}{L(b)} \right)^2 \langle v_l(\mathbf{x}_1, b) \cdot v_l(\mathbf{x}_2, b) \rangle = [s \cdot P(2s)]'_s, \quad (43)$$

$$R_{tt}(2s) = \left( \frac{b}{L(b)} \right)^2 \langle v_i(\mathbf{x}_1, b) \cdot v_i(\mathbf{x}_2, b) \rangle = P(2s), \quad (44)$$

where  $2s = |\mathbf{x}_1 - \mathbf{x}_2|/L(b)$  is the dimensionless distance between the points, and  $P(2s)$  equals (Gurbatov & Saichev 1981):

$$P(2s) = \frac{1}{\sqrt{2\pi}} \int_{-\infty}^{\infty} \frac{dz}{F(s+z) \exp\left[\frac{(s+z)^2}{2}\right] + F(s-z) \exp\left[\frac{(s-z)^2}{2}\right]}, \quad (45)$$

$$F(z) = \frac{1}{\sqrt{2\pi}} \int_{-\infty}^z \exp(-y^2/2) dy.$$

Now let us discuss the asymptotic behaviour of spectral and correlation properties of  $\mathbf{v}(\mathbf{x}, b)$  at  $b \gg b_0$ . The probability of finding two points in the same cell can be asymptotically expressed as:

$$P(s) = \begin{cases} 1 - \frac{s}{\sqrt{\pi}} & \text{at } 0 < s \ll 1 \\ \sqrt{\frac{\pi}{2}} \frac{1}{s} \exp\left(-\frac{s^2}{8}\right) & \text{at } s \gg 1 \end{cases}. \quad (46)$$

Thus, the correlation functions (43), (44) fall down quickly at large distances, i.e.,  $s \gg 1$ .

The correlation functions (43), (44) are non-analytic at  $s \rightarrow 0$  which is connected with breaks of the velocity field at  $v \rightarrow 0$ . The existence of breaks leads to the power-law asymptotic of the energy spectrum  $\sim k^{-2}$  at  $k \rightarrow \infty$ . However, this does not mean that the velocity field possesses a chaotic hierarchy of different scales. It is rather connected with the fact that a break of the field results in the appearance of many short waves in the spectrum, but their phases are correlated.

The probability-distribution function also keeps the information about the statistics of cell sizes. Indeed let us take an arbitrary straight line in space (e.g. one of the coordinates axes). Denote the intersection points of this line with walls of the structure as  $x_k$  and introduce the distribution function  $w(y)$  for dimensionless distances between the intersection points  $y_k = (x_k - x_{k-1})/L(b)$ . The function  $w(y)$  relates to  $P(s)$  by means of the following equation:

$$\langle y \rangle P(s) = \int_s^{\infty} (y-s) w(y) dy; \quad \langle y \rangle = \int_0^{\infty} y \cdot w(y) dy. \quad (47)$$

Combining this equation with (46), one obtains:

$$w(y) = \sqrt{\pi} P''(y), \quad \langle y \rangle = \sqrt{\pi}. \quad (48)$$

It is useful to compare  $w(y)$  with the distribution  $w_0(y) = \exp(-y)$  corresponding to random splitting of a straight line into intervals. The function  $w(y)$  falls down to zero at  $y \gg 1$  considerably faster than  $w_0(y)$ . This can be interpreted as the existence of order or coherent structure.

## 7 Discussion

A model is suggested describing approximately the late non-linear stage of gravitational instability in the Universe, dominated by some kind of weakly interacting dark matter. The main

purpose as well as application of the model is in the description of the general evolution of the large-scale structures in the Universe. The term 'large-scale structures' used here means the mass-density inhomogeneities which reached the non-linear regime  $\delta\rho/\rho > 1$ . In the present Universe the large-scale structures mean primarily clusters and superclusters as well as voids of galaxies. From a mathematical point of view, the model is based on Burgers' equation which has an analytical solution. This solution has an integral form (three-dimensional integral in the 3D case) but can be analysed from a geometrical and statistical point of view if one makes the additional assumption which, physically, means the neglect of cluster sizes as well as filament and pancake thickness. However, it can be used as a reasonable approximation for estimates of statistics of masses, spatial distribution and peculiar velocities of these objects. An essential advantage of the model is connected with the existence of an exact analytical solution of Burgers' equation. This allows one to avoid the 'step after step' numerical calculations in the cases when analytical analysis is impossible. Instead, one can calculate the mass distribution (of course with the restrictions mentioned above) at the epoch in question. In a sense this model is an extension of the well known Zel'dovich's approximation to the late non-linear stage, when the latter is not applicable.

According to the model under consideration, the basic quantity keeping the information about the late non-linear stage of density perturbation growth is the linear gravitational potential (i.e. the gravitational potential perturbations at the linear stage) rather than the linear-density perturbations. Of course, both of these quantities relate uniquely. However, they have different spectra:  $\Delta_k^2 \propto k^{-4} \delta_k^2$  (where  $\Delta_k^2$  is the spectrum of the potential perturbations and  $\delta_k^2$  is the spectrum of the density fluctuations), which results in different predictions for the evolution of statistical properties of the late non-linear objects.

### Acknowledgments

The English version of the paper was produced during a two month visit by SFS to the Max-Planck-Institut für Astrophysik. He thanks G. Börner, R. Kates and R. Klaffl for useful discussions of the problems related to the subject of the paper. He is especially grateful to T. Buchert for discussions and help.

### References

- Arnol'd, V. I., Shandarin, S. F. & Zel'dovich, Ya. B., 1982. *Geophys. Astrophys. Fluid Dynamics*, **20**, 111.  
 Bardeen, J. M., Bond, J. R., Kaiser, N. & Szalay, A. S., 1986. *Astrophys. J.*, **304**, 15.  
 Blumenthal, G. R., Faber, S. M., Primack, J. R. & Rees, M. J., 1984. *Nature*, **311**, 517.  
 Burgers, J. M., 1940. *Proc. R. Neth. Acad. Sci.*, **43**, 2.  
 Burgers, J. M., 1974. *The Nonlinear Diffusion Equation*. Reidel, Dordrecht.  
 Cole, J. D., 1951. *Quart. Appl. Math.*, **9**, 226.  
 Dekel, A., 1983. *Astrophys. J.*, **264**, 373.  
 Dekel, A. & Silk, J., 1986. *Astrophys. J.*, **303**, 39.  
 Doroshkevich, A. G., Kotok, E. V., Novikov, I. D., Polyudov, A. N., Shandarin, S. F. & Sigov, Yu. S., 1980. *Mon. Not. R. astr. Soc.*, **192**, 321.  
 Doroshkevich, A. G. & Zel'dovich, Ya. B., 1975. *Astrophys. Space Sci.*, **35**, 55.  
 Gurbatov, S. N. & Saichev, A. I., 1981. *Sov. Phys. JETP*, **53**, 347.  
 Gurbatov, S. N. & Saichev, A. I., 1984. *Isv. VUZ, Radiofizika*, **27** (in Russian).  
 Gurbatov, S. N., Saichev, A. I. & Shandarin, S. F., 1984. *Inst. Appl. Math.*, **152**, preprint (in Russian).  
 Gurbatov, S. N., Saichev, A. I. & Shandarin, S. F., 1985. *Sov. Phys. Dokl.*, **30**, 921.  
 Gurbatov, S. N., Saichev, A. I. & Yakushkin, I. G., 1983. *Sov. Phys. Usp.*, **26**, 857.  
 Hopf, C., 1950. *Comm. Pure Appl. Math.*, **3**, 201.  
 Kida, S., 1979. *Fluid Mech.*, **93**, 337.  
 Kofman, L. A. & Linde, A. D., 1987. *Nucl. Phys.*, **282**, 555.  
 Kofman, L. A. & Shandarin, S. F., 1988. *Nature*, **334**, 129.

- Kotok, E. V. & Shandarin, S. F., 1988. *Soviet Astr.*, in press.
- Kuznetsov, N. N. & Rozhdestvensky, B. L., 1961. *Zhurn. Vychisl. Mat. i Mat. Fiz.*, **1**, 217 (in Russian).
- Peacock, J. A. & Heavens, A. F., 1985. *Mon. Not. R. astr. Soc.*, **217**, 805.
- Peebles, P. J. E., 1980. *The Large Scale Structure of the Universe*, Princeton University Press, Princeton.
- Peebles, P. J. E., 1986. *Nature*, **321**, 27.
- Press, W. H. & Schechter, P., 1974. *Astrophys. J.*, **187**, 425.
- Primack, J., 1984. *Proc. Enrico Fermi*, **3387**, preprint.
- Rees, M. J., 1985. *Mon. Not. R. astr. Soc.*, **213**, 75p.
- Schaeffer, R. & Silk, J., 1985. *Astrophys. J.*, **292**, 319.
- Shandarin, S. F., 1988. In: *Large Scale Structures of the Universe*, p. 237, eds Audouze, J., Peletan, M. Ch. & Szalay, A., Kluwer, Dordrecht.
- Shandarin, S. F., Doroshkevich, A. G. & Zel'dovich, Ya. B., 1983. *Sov. Phys. Usp.*, **26**, 46.
- Tatsumi, T., 1980. *Adv. Appl. Mech.*, **20**, 39.
- White, S. D. M., 1987. In: *Nearly Normal Galaxies*, ed. Faber, S. M. Springer-Verlag.
- Zel'dovich, Ya. B., 1970. *Astr. Astrophys.*, **5**, 84.
- Zel'dovich, Ya. B., Mamaev, A. V. & Shandarin, S. F., 1983. *Sov. Phys. Usp.*, **26**, 77.